Open Access Journal

Journal of Power Technologies 92 (2) (2012) 68–79

journal homepage:papers.itc.pw.edu.pl

Computational study of an aerodynamic flow through a micro-turbine engine combustor

Marian Gieras *, Tomasz Stańkowski

Warsaw University of Technology
Nowowiejska 21/25, 00-665 Warsaw, Poland

Abstract

The study presents 3-D numerical simulations of aerodynamic flow inside a micro-turbine engine combustion chamber. The process of generating a numerical grid and its properties are described, and boundary conditions were determined on the basis of gas-dynamic calculation of the theoretical engine cycle. For the assumed boundary conditions, numerical simulations were performed of the aerodynamics of "cold" air flow through the combustion chamber (without fuel supply to the interior). A numerical experiment was also conducted which allowed the influence of the thermal energy supply into the combustion chamber on the aerodynamic flow through the chamber to be investigated. The work ends with a discussion of the results, in particular concerning the loss of pressure in the combustion chamber and possible design changes to minimize them..

Keywords: aerodynamic flow, engine combustor, pressure loss

1. Introduction

Micro-turbine engines are becoming widely used in many fields, e.g. models, unmanned aerial vehicles (UAVs), small-scale electricity generators or hybrid transport. The newest trends involve (i) miniaturization through a reduction in the size and weight of the engine, as well as an increase in the thrust to weight ratio, (ii) increased rotational speed of the turbo-compressor, and (iii) reduction in fuel consumption and emissions of harmful pollutants [1–7]. One of the main components of these engines is the combustion chamber. Several researchers have studied micro-turbine combustion [7–11], but none of these studies is able to give substantial information to further develop their design and technology. Knowledge of combustion processes in micro-turbine engines is mostly derived from full-scale testing of large turbine engines or basic research in simplified burners and combustion chambers. However, it should be noted that the miniaturization of engine construction leads to major changes in the parameters of the air flow and heat transfer in the engine. Therefore, in order to fully understand the problems associated with the miniaturization of gas turbine engines there is a need for numerical as well as experimental studies directly concerning these matters.

Computational fluid dynamics (CFD) is an attractive way to analyze this problem, not only for understanding the processes in the engine, but also for carrying out improvements and optimizations in terms of efficiency and pollutant emissions. However, no extensive work has been published using this tool [5, 6].

*Corresponding author

Email addresses: marian.gieras@itc.pw.edu.pl (Marian Gieras *), stankowski.tomasz@gmail.com (Tomasz Stańkowski)

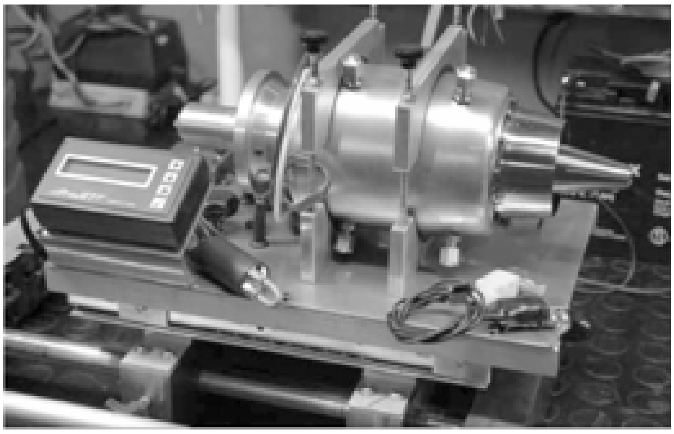

Figure 1: Photo of the GTM-120 turbo-jet engine

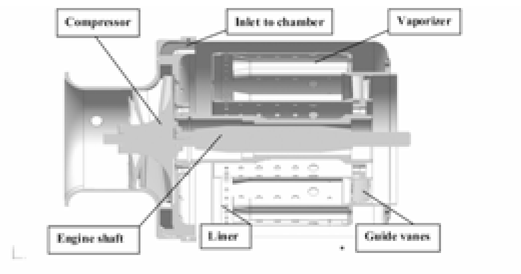

Figure 2: Cross-section along the length of the GTM-120 turbo-jet engine

In this paper 3-D numerical simulations were conducted of aerodynamic flow through the combustion chamber of a model GTM-120 turbojet engine. They represent the initial phase of the numerical calculations concerning the overall problems associated with the organization of combustion processes in the combustion chamber of this engine. In addition to experimental studies also conducted for this engine in the lab, it will be possible to optimize the construction of this engine in terms of minimizing fuel consumption and emissions of harmful pollutants while maximizing thermal efficiency.

2. GTM-120 turbo-jet engine

The engine GTM-120 is a single-spool, turbo-jet modeling engine. Fig. 1 shows a view of the engine mounted on a special test bed, which allows for measurement of the engine thrust. The main elements of the engine are: a one-stage centrifugal compressor, diffuser with special wedge-shaped inlet guide vanes, an annular combustion chamber with fuel vaporizer system (combustor) and a one stage axial turbine. The construction details of the GTM-120 engine are presented in Figs. 2 and 3.

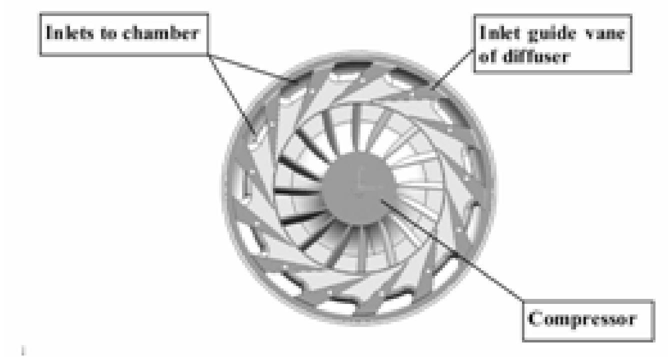

Figure 3: Cross-section of the GTM-120 turbo-jet engine showing the position of the compressor diffuser vanes

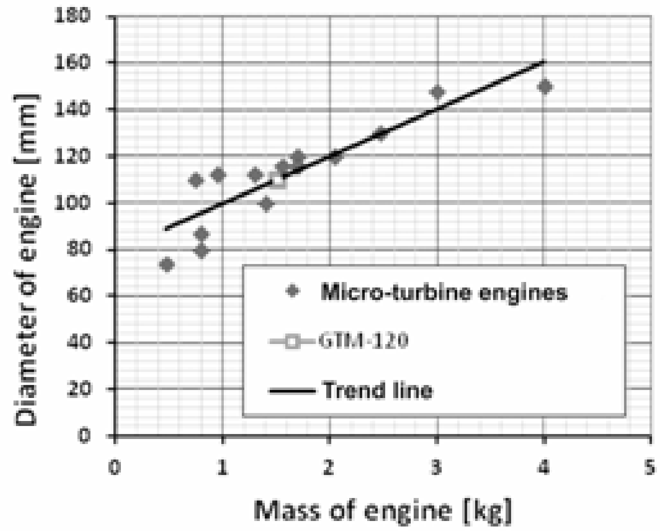

Figure 4: Diameter of engine versus mass of engine

Drawings of the engine have been made using Unigraphix NX 6.0 code. The basic dimensions and engine performance as obtained from the producer are provided in Table 1. It is worth noting that in terms of size, GTM-120 is strictly speaking in the class of miniature turbo-jet engines (Fig. 4).

2.1. Theoretical thermodynamic engine cycle

On the basis of the data received from the producer analytical calculations were made using turbo-jet engine theory [12, 13]. The design of the GTM-120 engine is treated in this case as a single-spool turbo-jet. Subsequent cross sections of characteristic designations were adopted according to the standard as: 1–inlet to the engine, 2–inlet to the compressor, 3–inlet

Table 1: The main parameters of the GTM-120 engine obtained from the producer

Parameter	Value	Unit
Weight of engine	1.5	kg
Maximum diameter of the front	110	mm
Length of engine	265	mm
Compressor diameter	70	mm
Engine inlet diameter	67	mm
Maximum rotational speed	120,000	rpm
Maximum engine thrust	120	N
Temperature of exhaust gas	870	K
Compression	2	-
Mass air flow	0.4	kg/s
Fuel consumption	400	ml/min

Table 2: Iteratively calculated input parameters

Parameter	Value	Unit
Inlet area of engine	0.0035	m^2
Atmospheric temperature	288	K
Atmospheric pressure	0.101	MPa
Air density	1.23	kg/m^3
Isentropic exponent of air	1.4	-
Gas constant of air	287	J/kg/K
Calorific value of fuel	42.8	MJ/kg
Isentropic exponent of exhaust gas	1.33	-
Exhaust gas constant	289	J/kg/K
Inlet pressure loss	0.03	-
Combustion chamber pressure loss	0.04	-
Efficiency of the compressor	0.78	-
Mechanical efficiency	0.99	-
Nozzle velocity loss coefficient	0.03	-
Coefficient amount of cooling air	0	-
Compression	2	-
Temperature before the turbine	1,008	K

section of the combustion chamber, 4–cross section of the inlet to the turbine, 5–the engine outlet. Prior to the calculations certain assumptions were made as to the estimation of loss factors in the individual segments of the engine. Due to the large number of input parameters, which required assumptions to be made, all calculations were carried out iteratively in MS Excel spreadsheet. Efforts were made to choose these parameters so as to obtain good agreement between producer data and the calculated values of engine thrust and air and fuel flow rate. The parameters obtained from the last iteration are shown in Table 2. A comparison between producer data and the results of calculations is presented in Table 3. It can be seen that maintaining compliance values of engine thrust and mass flow rate resulted in the need to increase the fuel flow rate. It can be assumed that the resulting values are correct, because the theoretical calculations of the thermodynamic cycle are performed for the maximum value, while the value of the fuel flow rate given by the producer is probably derived from averaging the instantaneous flow rate for different ranges of operation of the turbine engine. This analysis can be used to determine the approximate values of static parameters (pressure, temperature) in the typical cross-sections of the engine. These values are needed to estimate the boundary conditions necessary to carry out numerical simulations of air flow inside the combustion chamber. From this perspective, the following cross-sections are particularly interesting: 3–inlet of the combustion chamber and 4–outlet of the combustion chamber. These values are shown in Table 4.

3. Numerical simulation of aerodynamic flow through the combustor of the GTM-120 turbojet engine

3.1. Geometric model

The model GTM-120 engine was imported from the Unigraphix NX program to the Gambit program. This was followed by a slight simplification of the

Table 3: Comparison between the results of calculations and the data received from the producer

Quantities	Producer	Calculations	Unit
Thrust	120	120	N
Mass air flow rate	0.4	0.4	kg/s
Mass fuel flow rate	400	568	ml/min

Table 4: Approximate values of static parameters in the combustor (Cross-section)

	Unit	Inlet	Outlet
Area	m^2	0.00112	0.0028
Total temperature	K	369	1,008
Static temperature	K	342	978
Total pressure	MPa	1.97	1.89
Static pressure	MPa	1.50	1.67
Air density	kg/m^3	1.53	0.59
Velocity	m/s	234	246

Figure 5: Geometry of the combustion chamber prepared for numerical simulations

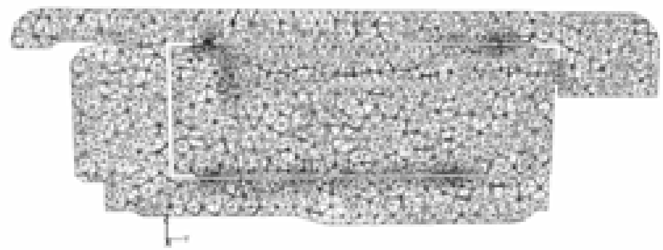

Figure 6: Discretization scheme of the combustion chamber

geometry by removing the screw holes and small curves in places that should not affect the results of the numerical simulation.

In engineering practice, the examination of the combustion chambers is carried out by the application of partial geometry models, using symmetry and periodicity models of a model. However, in this case, the model does not have symmetric or periodic characteristics. This can be seen in the combustion chamber, which has 12 vaporizers and 13 compressor guide vanes, and there is no plane of symmetry (Fig. 2 and 3). It was therefore decided to conduct a full 3-D geometry.

For the numerical simulations a mesh composed of tetrahedral elements was created. Tetrahedral mesh was chosen because of its ease in adjusting to the model geometry. In order to check the influence of grid density on the results of numerical simulations, basic calculations for two different grid densities were performed. The first numerical model assumed grid size in the range from 0.5 to 1.0 mm resulting in a total number of elements equal to 1 340 022. The smallest mesh size of 0.5 mm was used around the inlet holes to the combustor liner. The second model assumed grid size in the range from 0.5 to 0.7 mm resulting in a total number of elements equal to 1,835,780. Both numerical grid models satisfy the fundamental criterion of quality, where the skewness of the elements is less than 0.7 on a scale from 0 to 1.

Further improvement of the grid through appropriate simplification of the geometry and increasing the number of elements used in the simulation is certainly possible. However, at this stage of the calculations it is a compromise between computational time and accuracy of results. To obtain results with a convergence of mass flow below the level of 10-6 for such complex geometry over 2,000 iterations must be performed (each lasting no less than one minute with the use of a personal computer). This means that the computation time of one numerical simulation is about 35 hours.

The geometry of the combustion chamber prepared for numerical simulations is shown in Fig. 5.

The numerical model is presented in the Cartesian coordinate system in which the Y axis refers to the length of the engine. The surfaces of the inlet have been created as perpendicular to the direction of the air flow in the diffuser. This approach to the boundary conditions allowed a move away from the combustion chamber. It was necessary due to the methodology of modeling the inlet boundary conditions. Fig. 6 shows a cross-section of the plane X = 0, clear fine mesh around the inlet holes to the combustor liner and the inlet to the fuel vaporizers.

3.2. Boundary conditions

A high load condition was evaluated in this study. Air mass flow equal to 0.4 kg/s at the inlet and static pressure equal to $1.7 \cdot 10^5$ Pa at the outlet were assumed as the boundary conditions.

The software Ansys Fluent 12.1 solved the governing equations and other scalars in the turbulent flow. Second order discretization was used for all equations.

The selection of the turbulence model is a primary task in every CFD computation. Traditionally, the Reynolds Averaged Navier-Stokes turbulence model (RANS) has been used as a simplified engineering tool for aerodynamic flow and combustion issues. In the RANS model a time average or an ensemble average is calculated and turbulent structures are modeled. Alternatively, as explained by Boudier et al. [5] and James et al. [14], large eddy simulation (LES) seems to be the most appropriate approach to modeling combustion inside complex geometries. This is because LES is able to reproduce more accurately the turbulence, which plays a major role particularly in the combustion processes. In LES models only the scales below a specified filter length (sub-grid filter) are modeled.

The main drawback of LES, with respect to RANS, is a very long computational time when finer meshes and an unsteady solution are required. Choosing a turbulence model depends not only on the computational cost but also on a better description of the turbulence. In many cases, the use of a particular model may fail to converge, yielding unpredictable results.

Due to the computation time and convergence problems, to simulate aerodynamic flow through the combustion chamber of the turbo-jet engine Realizable a k-e (RANS) model was chosen. It is an enhanced version of the original standard turbulence model k-ε.

4. Numerical results

4.1. Model I

An assumption of a specific value of a static pressure at the surface of the outlet from the combustion chamber was selected in order to calculate the total pressure at the surface of the inlet for a given air flow through the combustion chamber. This assumption may be considered inconvenient in terms of comparing the results with those calculated for the theoretical thermodynamic cycle in this study. However, it has one advantage, namely, a boundary condition of the "MassFlow inlet" type guarantees the air mass flow given by the producer.

Using Fluent code a weighted average value of the parameter in the selected surface (inlet, outlet and space between the diffuser and combustion chamber) can be calculated. As a result of simulations, for example, the average total pressure at the inlet to the chamber equal to 0.233493 MPa and at the outlet of the chamber equal to 0.185405 MPa were obtained. Hence, in this case the total pressure drop in the combustor is equal to about 20%. It thus appears that the value of total pressure losses obtained from the numerical simulations is much higher than that projected for a turbo-jet engine (Table 2).

Fig. 7. presents a view of the contours of the Mach number in the section y = 0.04 in the diffuser of the compressor. It can be found that in the inlet part of the diffuser a relatively high speed in the range from 0.7 to 0.8 Mach is achieved. An excessive increase in velocity is caused by an overly high air mass flow through the surface of the inlet, which may indicate that the air flow is too damped at the inlet to the diffuser. A contour map of velocity in the cross-section X = 0 is given in Fig. 8. This map allows one to observe the relevant directions of air flow inside the chamber. Part of the air flows through the annular channel and enters the chamber through a row of holes in the inner and outer liner wall. The rest of the air travels along the liner outside wall to the end where it turns and enters the center of the liner

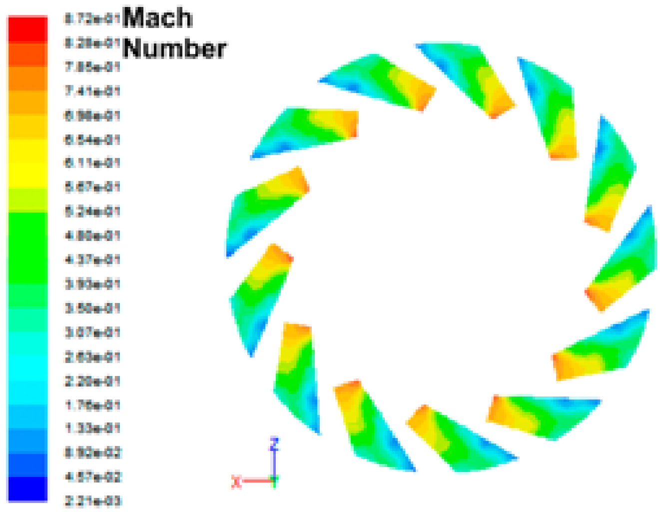

Figure 7: Contours of Mach Number in the diffuser

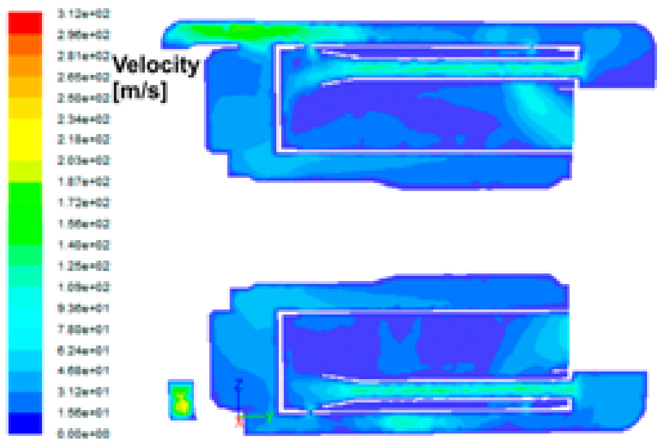

Figure 8: Contours of velocity magnitude in the combustor

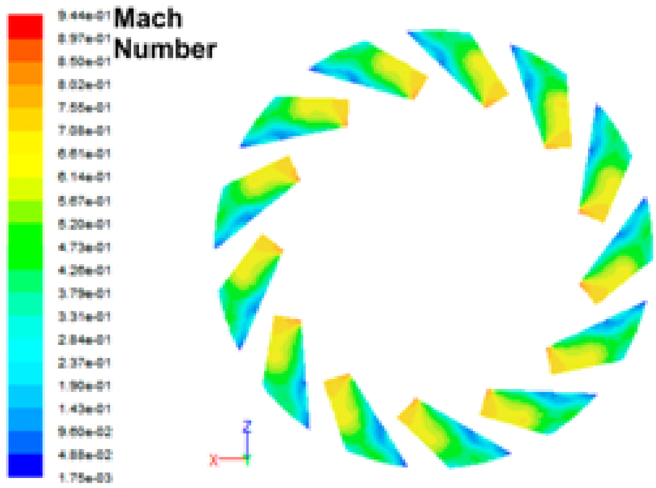

Figure 9: Contours of Mach Number in the diffuser

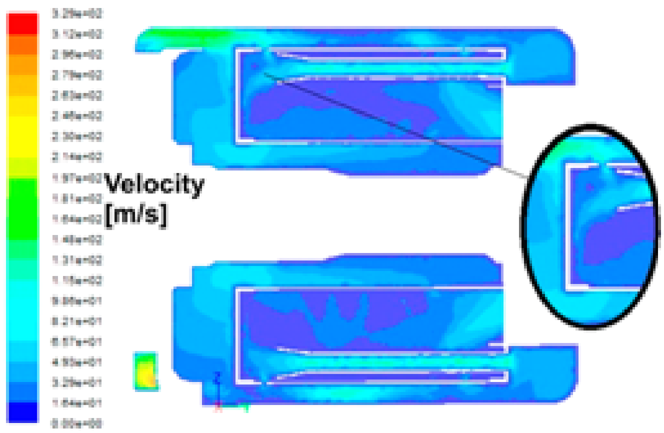

Figure 10: Contours of velocity magnitude inside combustor

through the tubular vaporizer. Organizing the aerodynamic flow in this way and placing the fuel pipes at the beginning of the vaporizer should deliver good evaporation and stable combustion of the fuel.

4.2. *Model II*

The numerical calculations carried out for a more fine mesh show that increasing mesh density does not cause significant changes in the nature of the phenomena occurring inside the combustor. Very similar velocity distribution in the diffuser (in the range from 0.7 to 0.85 Mach, Fig. 9) as well as inside the combustor (Fig. 10) was obtained. Increasing the mesh density resulted only in slight changes in average values, among others a local increase in total pressure at the inlet (from 0.233493 MPa to 0.239324 MPa) and outlet (from 0.185405 MPa to 0.186760 MPa). Hence, it can be calculated that the total pressure loss in the combustor also remains at a similar level.

4.3. *Model III*

Overly high air velocity at the inlet to the diffuser and excessively large total pressure losses in the combustor obtained from numerical simulations for the specified assumptions in relation to the expected value [1, 15–18] resulted in a change in the approach to analysis of the study of aerodynamics inside the combustor. It was decided to carry out numerical simulations for the amount of air mass flow resulting from the analysis of trends for this type of model turbo-jet engine (Fig. 11). Fig. 11 shows that the average value of air mass flow turbo-jet engines of the same mass as the GTM 120 engine oscillates around

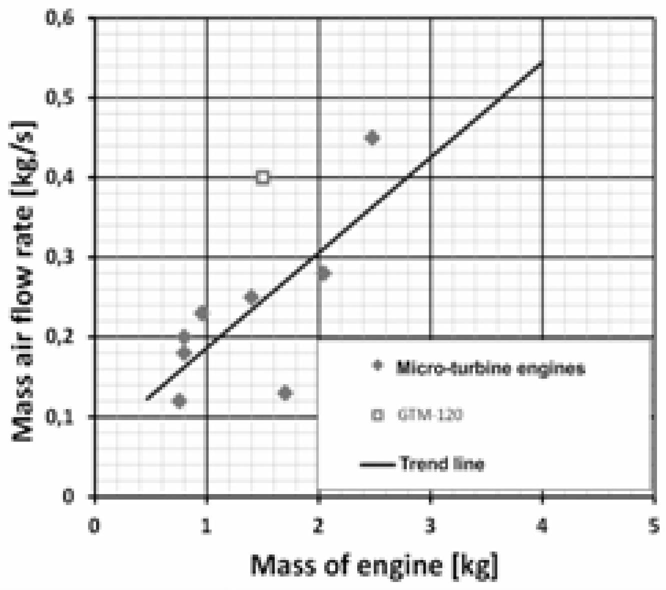

Figure 11: Air mass flow versus mass of different micro-turbine engines

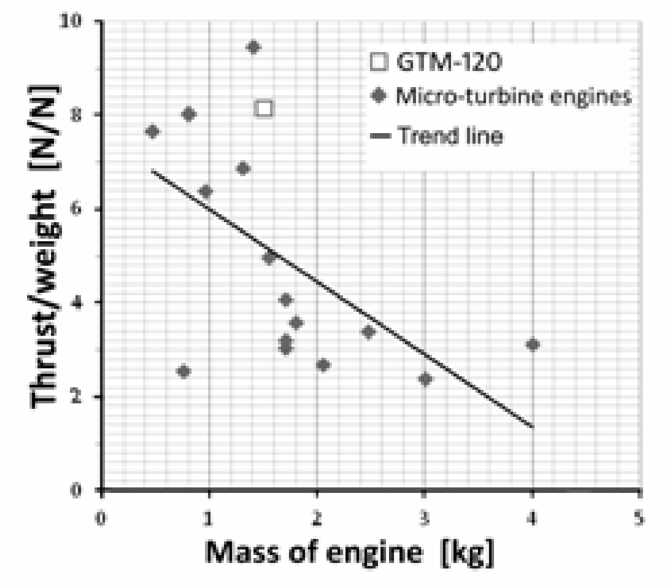

Figure 12: Thrust-weight ratio versus mass of engine

the value of 0.25 kg/s. For this value of mass flow and for the slightly increased values of total pressure losses in the combustor equal to 6% (due to correction resulting from the miniaturization of the engine) a new theoretical cycle of the turbo-jet engine was calculated. As a result of gas-dynamic calculations a new value of engine thrust equal to 88 N was obtained which, for the analysis of trends (Fig. 12), was in line with expectations. A similar value of thrust (90 N) was obtained by using an NS–6 strain gauge force sensor during a laboratory test for this engine. This may indicate that the actual value of the engine air flow is closer to 0.25 kg/s than to the 0.4 kg/s given by the producer. Additionally, the total pressure at the inlet to the combustion chamber of 0.202655 MPa and at the outlet of the chamber of 0.190496 MPa was calculated. Thus, it was possible to determine the new boundary conditions for numerical simulations.

Numerical simulations were performed for a finer 0.7 mm mesh. In the area of the inlet to the chamber a finer grid with dimensions of 0.5 mm was also used. This resulted in the total number of elements being 1,835,780. The basic settings of the Ansys Fluent solver were left unchanged. The boundary conditions were set as follows:

- mass flow of air at the inlet (Mass Flow inlet) of 0.25 kg/s
- static pressure at the outlet (Pressure Outlet) of $1.7 \cdot 10^5$ Pa.

Previously, for air mass flow of 0.4 kg/s, the most problematic issue was the flow through an area of the diffuser vanes rim of the compressor. In the simulations carried out at a reduced mass flow rate value for the newly-chosen boundary conditions for pressure, total pressure values were obtained similar to those obtained from theoretical cycle calculations. Another beneficial effect of the changes is the reduction of the Mach number in the diffuser. Previously obtained velocity values were not very good (close to the speed of sound) due to both the rapid increase in pressure loss and the problems associated with numerical modeling.

In this case, the Mach number at the intake is about 0.5 which then decreases along the diffuser to values at which sound effects are negligible. For this reason, numerical simulations based on this boundary condition are more correct. In large engines the flow velocity in the combustion chamber does not usually exceed 0.3 Mach, which often allows one to model numerically the flow as incompressible. Since in the case analyzed here, there are areas of high speed, a compressible model remains unchanged. In this model the working medium, air, is treated as an ideal gas, (which in itself is an approximation).

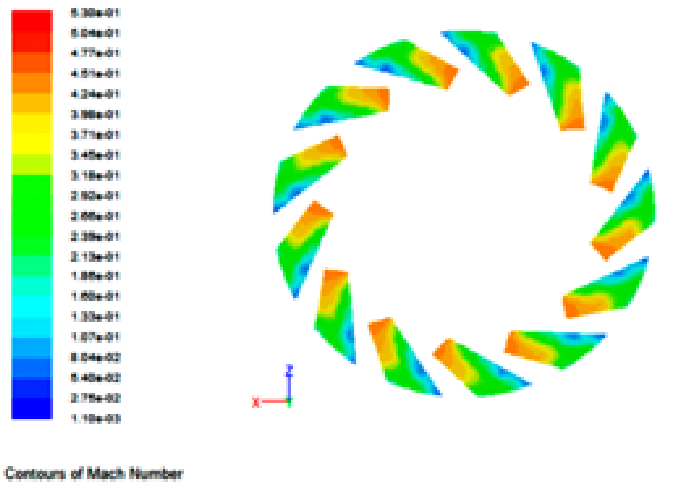

Figure 13: Contours of Mach number in the diffuser

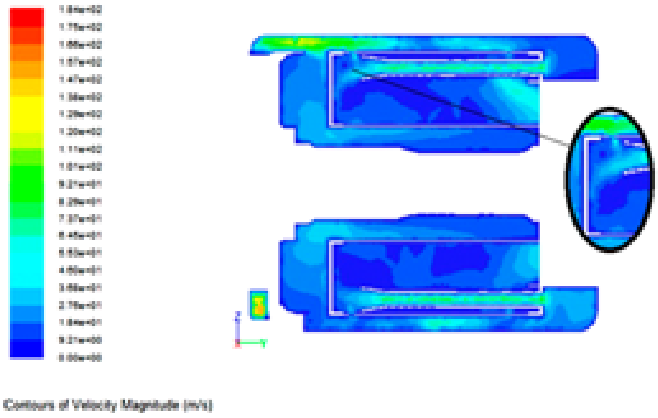

Figure 14: Contours of velocity magnitude in the combustor

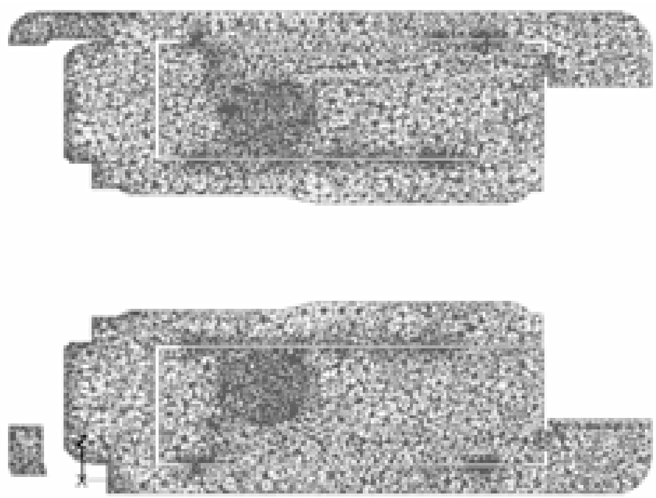

Figure 15: A view of the numerical grid for the cross-section X = 0

The Mach number values in the compressor section of the diffuser are shown in Fig. 13. It should be noted that the flow falls to about 0.2 Mach after going a short distance in the diffuser, which is beneficial both for the further distribution of the flow in the combustion chamber, as well as due to the chosen method of flow modeling.

By reducing the mass flow and thus reducing flow velocity, the pressure loss in the combustor was also reduced. And so in the inlet section of the combustor just behind the diffuser, (for the section y = 0.01 m), a total pressure drop inside the combustion chamber of 10% was obtained. The value drawn from the literature is between 4% and 8% for typical combustion chambers larger than the chamber being modeled. The resulting 10% in this case, on the one hand, indicates increased losses in the chamber associated with miniaturization of the engine, and on the other hand, shows the possibility of optimizing the chamber to obtain a more favorable value.

Fig. 14 shows the velocity distribution inside the combustion chamber. The obtained values of velocity are much better and more appropriate for the organization and stabilization of combustion processes. For example, the average velocity in the cross section y = 0.01 is about 100 m/s. In the combustion chamber, in areas in which combustion takes place the velocity range is from zero to several m/s. At the outlet of the combustor leading to the blade rim of a turbine the average speed reaches about 40 m/s (for cold flow).

4.4. Model IV

In order to better approximate the actual distribution of air flow through the combustion chamber the numerical simulations of a flow with an additional heat source were carried out. At this stage of research discussions about changes in the distribution of velocity and pressure of air flow through the combustion chamber caused by the placement of heat sources inside the chamber were carried out. The main purpose of this simple numerical experiment was merely to verify whether the addition into the combustion chamber of a certain amount of heat (in a form similar to the actual conditions existing in the chamber) caused any additional interference and disturbance of aerodynamic flow through the combustion chamber. For the modeling of the internal heat source, it was necessary to create a new internal volume in the combustor liner. Inside the annular combustor the most suitable area for modeling is the torus, located in the area with the greatest heat emission. A new grid was prepared, which again uses tetrahedral elements of 1 mm in size. As before, a finer grid was used near the inlet to the liner. Finally, the mesh, consisting of 1.79 million volume elements was obtained. A view of the numerical grid for the cross section X = 0 is shown in Figure 15.

The assumed value of air mass flow rate is 0.25 kg/s, while the required static pressure at the output of combustor is $1.7 \cdot 10^5$ Pa. In this case, the additional boundary condition is to determine the value of the heat source temperature. It was assumed that the entire area of the modeled torus has a temperature of 2500 K. The temperature of exhaust gas in the primary zone of the combustion chamber of turbo-jet engines normally ranges between 2,150 and 2,450 K [15–19]. A slightly higher value was adopted because of the limited size of the heat exchange surface. In fact, it is expected that the combustion process will occur on a much larger area. The assumption of a constant temperature in a given area resulted in the emission of a heat flow with a value of 78,390 J/s into the combustion chamber. This value is about one-fourth of the maximum theoretical value calculated for the GTM-120 turbo-jet engine (due to the limited size of the area in which the heat is emitted). However, it should also be noted that in this case the net heat flow value is used without taking into account the heat losses.

Fig. 16 shows a section in the plane X = 0 m, which contains the temperature distributions. For heat distribution across the engine, it can be observed that the highest temperature is concentrated in the area emitting heat, which is drawn out in the direction of the outlet.

The temperature distribution in cross-sections of the combustion chamber is very interesting. In Fig. 17 it can be seen that as the air flowing through the holes in the liner creates an air film at a liner wall insulating it from contact with hot air. It can also be seen that the hot air flows around the fuel vaporizers through which heat is transported to the interior, causing heating and evaporation of fuel flowing inside. Then, later in the combustion chamber, temperature equalization occurs by providing additional cool air from an external annular channel by special dilution holes.

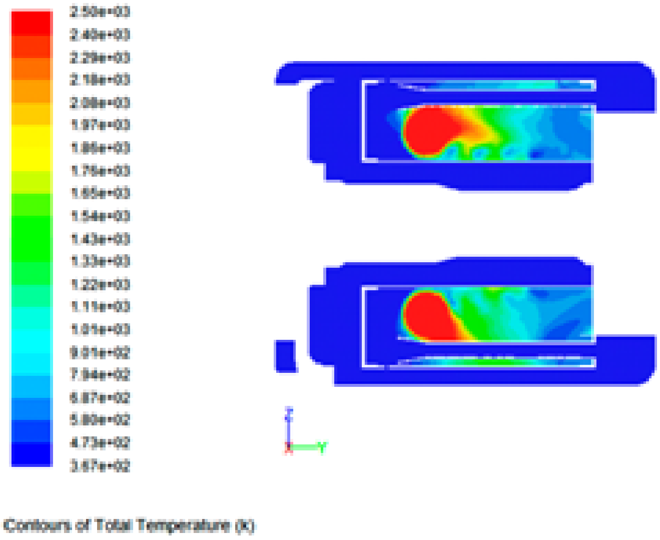

Figure 16: Contours of temperature in the combustor

In the present case, flow velocity difference between the front and the rear of the combustor liner is greater than in the cases performed without the heat source. At the front, the velocity is estimated as being from 0 to about 10 m/s, while at the end of the liner it reaches about 100 m/s (Fig. 18). Such a rapid increase in velocity results in a change of static pressure, the value of which at the end of the combustion chamber must be reduced relative to the rest of the chamber.

5. Discussion of results

Aerodynamic processes play a crucial role in the design and performance of turbo-jet engine combustion systems. Successful aerodynamic design demands knowledge of flow recirculation, jet penetration and mixing. The purpose of the work is to show (using the example of the GTM 120 turbo-jet engine), how the air flowing through the combustion chamber of a small turbine engine is shaped, where the critical places of the flow are and what the relationships between air mass flow and pressure losses are. In the diffuser and annulus the main objectives are to reduce the flow velocity and to distribute the air in prescribed amounts to all combustor zones.

The numerical simulations show that a compressor diffuser, which ends with a narrow air inlet chan-

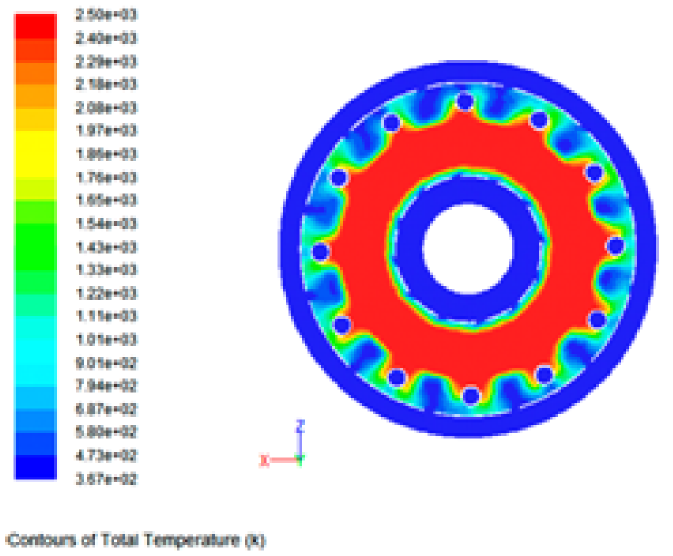

Figure 17: Contours of temperature in cross sections of the combustor

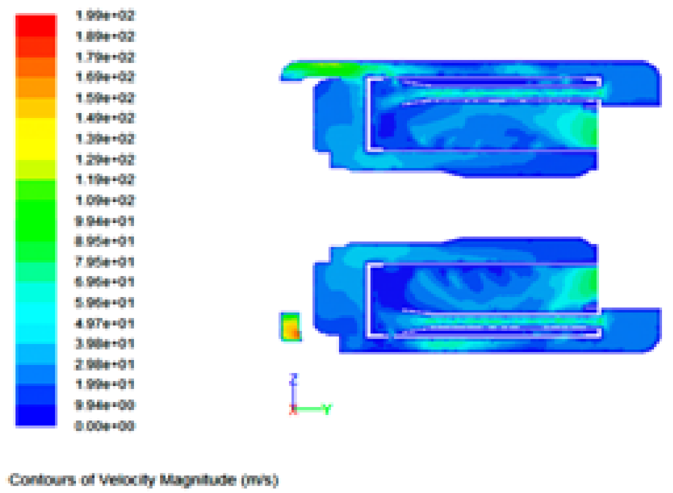

Figure 18: Contours of velocity magnitude in the combustor

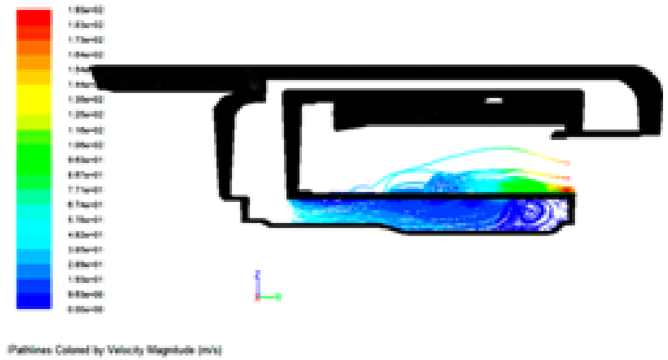

Figure 19: Pathlines of velocity magnitude showing the air flow through the annulus and through the second row of holes into the liner

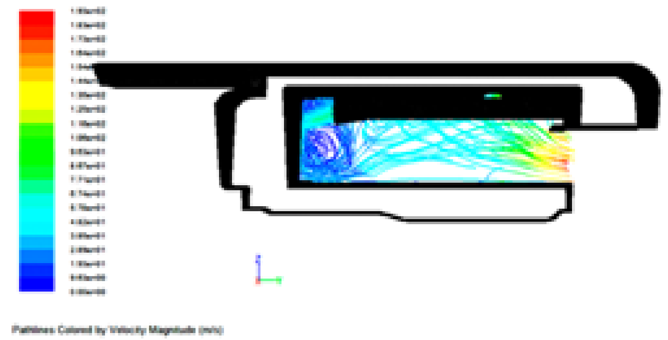

Figure 20: Pathlines of velocity magnitude in the liner

nel to the combustion chamber, plays an important role in generating the pressure loss (Figs. 7, 9 and 13). The size and shape of these channels give rise to the high speed and non-uniformity of a flow, which are an important source of pressure loss. The consequence of excessive flow velocity in the diffuser and the annulus may also restrict the flow through the first row of holes in the combustion chamber. Consequently, the deterioration process of mixing fuel with air may take place. This phenomenon is illustrated in Fig. 19 where pathlines of the fluid elements in the annulus of the combustion chamber are presented. It is seen that, as a result of deviations in the direction of flow from the duct wall, most of the fluid elements bypass the first row of inlet holes to the liner. This negative effect can probably be corrected by reducing the flow velocity in the annular channel and by modifying the shape of this channel.

Analyzing the velocity distribution inside the combustion chamber, one can identify areas inside the liner with a speed of less than one meter per second and areas with visible turbulence, which occurs primarily in the area between the outlet of the vaporizer and the central part of the liner interior (Figs. 8, 10, 14, 18). The presence of these areas is particularly important due to combustion processes, since for a stable fuel burning process an adequately low established flow velocity is required: this way the flame is not blown out and the new fuel-air mixture has an adequate contact time with the residue gas in the chamber.

Based on analysis of the velocity contours shown in Figs. 8, 10, 14 and 18, it can be concluded that the change in air mass flow and the placing of a heat source in this area do not cause major changes in the size and shape of the gas recirculation zone. To better illustrate this zone, pathlines of velocity magnitude inside the liner are shown in Fig. 20. The Figure shows that the zone is in accordance with accepted canons located in front of the combustor, where it forms the primary combustion zone. This allows fuel that was not completely burned in this zone, to be burned in the next section of the combustor.

It may also be noted that the velocity at the outlet of the chamber is much lower than that estimated by the gas-dynamic calculations. However, one should remember that the subject of discussion in this work is an aerodynamic flow through the combustor which does not include supplies of fuel and combustion modeling. In this case combustion modeling could provide more accurate results. A relatively simple numerical experiment, involving the insertion of heat source in the recirculation zone showed a marked improvement in the flow velocity distribution in the combustor. That involved maintaining a low velocity in front of the chamber followed by a significant increase in velocity at the outlet from the chamber to a value of approximately 100 m/s (Fig. 18).

The numerical simulations show that relatively large losses of total pressure in the combustor are caused by the air flowing through many narrow channels, and by sudden turns in the direction of the flow, which both contribute to the growth of the boundary layer and the formation of a local turbulence, choking the flow. It can be assumed that the connection of the numerical calculations with experimental studies on the GTM 120 turbo-jet engine will contribute to a more optimal design of this engine.

6. Summary and conclusion

From the conducted numerical simulations the following conclusions can be drawn:

- the total pressure loss in this type of miniature combustor (cold flow) is approximately 10%,
- the increase in the mass flow of air through the combustor causes a sharp increase in the total loss of total pressure,
- to obtain a smaller loss of pressure it is necessary to optimize the geometry of the whole combustion chamber,
- the addition of a certain amount of heat to the combustor does not cause disturbance to the aerodynamic flow within the chamber, while the effect on the profile of the outlet velocity, temperature and air density is clearly visible,
- the Reynolds averaged Navier-Stokes turbulence model (RANS) seems to be a relatively good, simplified engineering tool which can be used for preliminary numerical simulations of an aerodynamic flow and combustion problems.

References

[1] T. Kamps, Model Jet Engines, Traplet Publications Ltd (2005).

[2] K. Schreckling, Home Built Model Turbines, Traplet Publications Ltd (2005).

[3] K. Schreckling, Gas Turbines for Model Aircraft, Traplet Publications Ltd (2003).

[4] B. F. Kolanowski, Guide to Microturbines, Fairmont Press (2004).

[5] G. Bouldier, L. Y. M. Gicquel, T. Poinsot, D. Bissieres, C. Berat, Comparison of les, rans and experiments in aeronautical gasturbine combustion chamber, Proceedings of the Combustion Institute 31 (2) (2007) 3075–3082.

[6] C. A. Gonzales, K. C. Wong, S. Armfield, Computational study of a micro-turbine engine combustor using large eddy simulation and reynolds average turbulence models, ANIZAM Journal 49 (2008) 407–422.

[7] P. D. Marsh, Rcu review: Twenty years of micro-turbojet engines, Magazine Horizon (2003) 1–8.

[8] M. D. Agrawal, S. Bharani, Performance evaluation of a reverse-flow gas turbine combustor using modified hydraulic analogy, Journal MC 85 (2004) 34–44.

[9] H. S. Lee, J. J. Yoon, The study on development of low nox combustor with lean burn characteristics for 20 kw class microturbine, in: Proceedings of ASME Turbo Expo, Vienna, Austria, 2004.

[10] R. Tuccillo, M. C. Cameretti, Comparing different solutions for the micro-gas turbine combustor, in: Proceedings of ASME Turbo Expo, Viena, Austria, 2004.

[11] S. Adahia, A. Iwamotoa, S. Hayashib, H. Yamadab, S. Kaneko, Emissions in combustion of lean methane-air and biomass-air mixtures supported by primary hot burned gas in multi-stage gas turbine combustor, Proceedings of the Combustion Institute 31 (2) (2007) 3131–3138.

[12] S. Antas, P. Wolański, Obliczenia termogazodynamiczne lotniczych silników turbinowych, Wydawnictwo Politechniki Warszawskiej, Warszawa, 1989.

[13] P. Dzierżanowski, Turbinowe silniki odrzutowe, Wydawnictwa Łączności i Komunikacji, Warszawa, 1983.

[14] S. James, J. Zhu, M. Anand, Large-eddy simulation as a gas turbine combustor at different pressure and swirl conditions, Applied Thermal Engineering 19 (19) (1999) 949–967.

[15] M. Gieras, Komory spalania silników turbinowych, organizacja procesu spalania, Oficyna Wydawnicza Politechniki Warszawskiej, Warszawa, 2010.

[16] A. H. Lefebvre, Gas Turbine Combustion, Taylor & Francis, 1999.

[17] K. Hunecke, Fundamentals of Theory, Design and Operation, Motorbooks, International Publishers and Wholesalers, 1997.

[18] R. Łapucha, Komory spalania silników turboodrzutowych, Wydawnictwa Naukowe Instytutu Lotnictwa, Warszawa, 2004.

[19] J. D. Mattingly, Aircraft Engine Design, American Institute of Aeronautics and Astronautics, 2002.